A comparison of Bandwidth in RCE-SAGCM-APD and WG-SACM-APD structures, based on PSPICE model

N. Lotfivand [a] and H. Rasooli Saghai [b]

a) Department of Electrical Engineering, Islamic Azad University of Tabriz, Tabriz, Iran
E-mail: ahoora4444@hotmail.com

b) Department of Electrical Engineering, Islamic Azad University of Tabriz, Tabriz, Iran
E-mail: h_rasooli_s@yahoo.com

Abstract:

In this paper, a proper circuit models based on "Carrier time – domain transport process" in two important APD photodetector structures: RCE – SAGCM-APD and WG-SACM-APD are presented. These circuit models are studied for frequency responses of these two devices as well as how these responses depend on physical characteristics of the device such as: absorption layer thickness, multiplication layer thickness and multiplication gain. Finally, a comparision is made between the bandwidth limitations of these two devices.

Keyword:

RCE – SAGCM-APD, WG-SACM-APD, and circuit model.

I. INTRODUCTION

For develop high-performance optoelectonic integrated circuits (OEICs), high-speed photodetectors are an essential component . Two important characteristics of a high-performance photodetector are its quantum efficiency (QE) and its bandwidth(BW). These two characteristics usually act inverse each other. For tradeoff between the bandwidth and the quantum efficiency two structures Fabry–Pérot resonant-cavity and waveguide are presented . [1],[2]
Avalanche photodiodes (APDs) between conventional photodetector structures are attractive for fiber-optic communication systems due to the significant improvement in sensitivities afforded by their internal gains.

To achieve a high-performance structure, a low electric field in absorption regions and a high electric field in the multiplication layer is essential and this can be achieved by using a highly doped charge layer, between avalanche and absorption regions .This structure are called separate absorption grading charge multiplication APD (SAGCM-APD) .[3] By tradeoff between the bandwidth and the quantum efficiency photo detecting can be done. That structure can be used in developed form with Resonant Cavity Enhanced - Separated Absorption Graded Charge Multiplication-Avalanche Photodetector (RCE-SAGCM-APD) or Waveguide Separated Absorption Charge Multiplication Avalanche Photodetector (WG-SACM- APD). [2] ,[3]

In this work, we discuss photo-generated and transfer carriers on the RCE-SAGCM-APD and the WG-SACM-APD structures for obtain transfer function according the frequency response .In the SPICE modeling, we have studied the effects of the bandwidth and physical characteristics on the structures . Finally, by results the bandwidth limiting in both structures is compared.

II. TRANSFER FUNCTION CALCULATION

A. *THE RCE-SAGCM-APD*

A schematic structure of the RCE-SAGCM-APD is shown in Fig. 1. The total optical power in the absorption layer of the RCE-APD is the sum of the optical power of the forward and backward light waves. The forward wave comes from the top mirror while the backward wave is that reflected from the bottom mirror of the cavity. Hence, the forward quantum efficiency, η_f , is the ratio between the forward optical power to the incident power, and it is calculated from : [3]

$$\eta_f = \frac{(1-R_1)[1-\exp(-\alpha x_a)]}{[1-\sqrt{R_1 R_2}\exp(-\alpha x_a)]^2} \quad (1)$$
$$= \eta_f^*[1-\exp(-\alpha x_a)]$$

Similarly, the backward quantum efficiency, η_b is :

$$\eta_b = \frac{(1-R_1)[R_2\exp(-\alpha x_a)][1-\exp(-\alpha x_a)]}{[1-\sqrt{R_1 R_2}\exp(-\alpha x_a)]^2} \quad (2)$$
$$= \eta_b^*[1-\exp(-\alpha x_a)]$$

The reflectivity of the top mirror (R_1) should satisfy the condition of constructive interference at the absorption layer [3],

$$R_1 = R_2\exp(-2\alpha x_a) \quad (3)$$

In the above equations, the standing wave effect (SWE) is taken into consideration in terms of the absorption coefficient, as it is expressed as :

$$\alpha = \alpha_0 \cdot SWE \quad (4)$$

where is the absorption coefficient of the active layer of the photodetector SWE [4] is expressed as :

$$SWE = 1 + \frac{2\sqrt{R_2}}{\beta x_a(t+R_2)} Sin(\beta x_a) \quad (5)$$

When the incident radiation is absorbed in the absorption region,electron-hole pairs are generated. To calculate the impulse response of the photodetector, the concentration of the photogenerated carriers as a function of time is required. After the photogenerated electrons travel the dead space length ($\Delta\omega_m$) inside the multiplication region, the secondary generation of electrons and holes starts. Both the primary and secondary photogenerated electrons moves toward the N^+ layer, while the primary and secondary photogenerated holes move to the P^+ layer, resulting in the photogenerated current.[5],[6] An equivalent circuit is presented in Fig. 3(a). The transfer function H is calculated according to the frequency response .[7] H_p and H_s are the components of that represent the effects of the primary and secondary hotogenerations, respectively. These components are given by :

$$H_p(\omega) = \{(\eta_b^* + \eta_f^*)\frac{1-\exp(-\alpha x_a)}{j\omega} \quad (6)$$
$$\times(v_n[1-\exp(-j\omega\frac{x_t+x_d}{v_n})] + v_p[1-\exp(-j\omega\frac{x_{g_1}}{v_p})])$$
$$+\frac{1}{j\omega}(v_n\exp(-j\omega\frac{x_t+x_d}{v_n})$$
$$\times[1-\exp(-j\omega\frac{x_a}{v_n})][\eta_f^* - \eta_b^*\exp(-\alpha x_a)]$$
$$+v_p\exp(-j\omega\frac{x_{g_1}}{v_n})][1-\exp(-j\omega\frac{x_a}{v_p})]$$
$$\times[u_b^* - u_f^*\exp(-\alpha x_a)])$$
$$+v_n\exp(-j\omega\frac{x_t+x_d}{v_n})$$
$$\times(\frac{\eta_f^*}{\alpha v_n - j\omega}[\exp(-\alpha x_a) - \exp(-j\omega\frac{x_a}{v_n})]$$
$$+\frac{\eta_b^*}{\alpha v_n + j\omega}[1-\exp(-\alpha x_a - j\omega\frac{x_a}{v_n})])$$
$$+v_p\exp(-j\omega\frac{x_{g_1}}{v_p})$$
$$\times(\frac{\eta_b^*}{\alpha v_p - j\omega}[\exp(-\alpha x_a) - \exp(-j\omega\frac{x_a}{v_n})]$$
$$+\frac{\eta_f^*}{\alpha v_p + j\omega}\times[1-\exp(-\alpha x_a - j\omega\frac{x_a}{v_p})])\}$$

$$H_s(\omega) = [\frac{M_0 - 1}{1 + j\omega(M_0-1)\tau_m}] \quad (7)$$
$$\times\{\eta_f^*[\frac{1}{j\omega} - \frac{1}{j\omega - \alpha v_n}]$$
$$\times[\exp(-\alpha x_a) - \exp(-j\omega\frac{x_a}{v_n})] - \eta_b^*[\frac{1}{j\omega} - \frac{1}{j\omega + \alpha v_n}]$$
$$\times[1-\exp(-\alpha x_a - j\omega\frac{x_a}{v_n})]\}$$
$$\times(v_n\exp(-j\omega\frac{x_t}{v_n})$$
$$\times[\exp(-j\omega\frac{x_d}{v_n}) - \exp(-j\omega\frac{\Delta\omega_m}{v_n})]$$
$$-v_p\exp(-j\omega\frac{x_t+\Delta\omega_m}{v_n})$$
$$\times[1-\exp\times(-j\omega\frac{x_{g_1}+x_t+x_a+\Delta\omega_m}{v_p})])$$

The total transfer function H is calculated from:

$$H(\omega) = \frac{H_s(\omega)+H_p(\omega)}{\omega_t} \quad (8)$$

Where ω_t is:

$$\omega_t = x_{g_1} + x_a + x_{g_2} + x_c + x_d \quad (9)$$

The output current from the photodetector is then :

$$I_{out}(\omega) = \frac{i_{ph}H(\omega)}{(1-\omega^2 LC_d + j\omega RC_d)} \quad (10)$$

The capacitance of the photodetector, C_d , is composed of the series capacitances of the different layers of the photodetector .

In Fig. 3(b), a PSPICE representation of this model is shown. Here, a voltage source instead of the optical current source is used. Then the output voltage is transformed to a current through the voltage-controlled current source and applied to the load and the parasitic elements R_d and C_d to get the frequency response . [7]

B. ***THE WG-SACM-APD***

A schematicstructure of a waveguide separated absorption charge multiplication avalanche photodetector (WG-SACM-APD) is shown in Fig. 2. In WGPDs, the photon flux and carrier transport directions are perpendicular to each other and hence the bandwidth and the quantum efficiency can be specified almost independently of each other. Further, the lateral illumination from the side of the photodetector means that the quantum efficiency is a function of the length of the absorption layer and not its thickness. Therefore, with a long and thin absorption layer, both high quantum efficiency that depends on its length and low transit time that depends on its thickness can be simultaneously achieved. [8]

The lateral incident optical signal on the absorption layer of the photodetector generates the primary electron-hole pairs. The transfer function obtained by calculating the Fourier transform of time response. [8]

$$H(\omega) = H_s(\omega) + H_p(\omega) \qquad (11)$$

$$H_p(\omega) = \frac{\eta}{\omega_t}\{\frac{v_n + v_p}{j\omega} + \frac{1}{\omega^2 x_a}[v_n^2(1-\exp(-\frac{j\omega x_a}{v_n}))$$
$$\times\exp(-\frac{j\omega(x_t + x_d)}{v_n}) + v_p^2(1-\exp(-\frac{j\omega x_a}{v_p}))]\} \qquad (12)$$

$$H_s(\omega) = \frac{\eta}{\omega_t}(\frac{M_0 - 1}{1 + j\omega\tau_m(M_0 - 1)})(\frac{v_n}{x_a\omega^2}) \qquad (13)$$
$$\times[1-\exp(-\frac{j\omega x_a}{v_n})]\exp(-\frac{j\omega x_t}{v_n})$$
$$\times\{v_n[\exp(-\frac{j\,\omega x_d}{v_n}) - \exp(-\frac{j\,\omega\Delta\omega_m}{v_n})]$$
$$+v_p\exp(-\frac{j\,\omega\Delta\omega_m}{v_n})$$
$$\times[\exp(-\frac{j\omega(x_a + x_t + \Delta\omega_m)}{v_p}) - 1]\}$$

In the above equations η is the quantum efficiency of the waveguide photodetector that can be expressed as

$$\eta = K(1-R)(1-\exp(-\alpha\Gamma L)) \qquad (14)$$

where K is the coupling efficiency, R is the reflectivity of the photodetector, α is the absorption coefficient of the absorption region, Γ is the confinement factor of the absorption layer and l is the length of the absorption layer.

$$x_t = x_{g_2} + x_c \qquad (15)$$

The extrinsic response of the photodetector depends on both the photogenerated carriers and the parasitics elements of the photodetector. Hence, the output extrinsic current is expressed as

$$I_{out}(\omega) = \frac{qp_i}{hv}\frac{H(\omega)}{1 + j\omega C_d R_{tot} - \omega^2 C_d L_s} \qquad (16)$$

The circuit model for this structure is like Fig. 3 but with own transfer function

III. SIMULATION

Simulated results, for both structures using the parameters of the photodetectors listed in Tables I. In Fig. 4 and Fig. 5 the multiplication factor -bandwidth characteristics of the photodetector is plotted for different area. As shown in this figures , an increase in the multiplication factor results in an decrease of bandwidth because by increasing multiplication gain, the number of the photogenerated primary carriers and the photocurrent increases. resulting in an increase of the transit time and hence a decrease of the bandwidth of the photodetector.

The effect of the area of the multiplication layer is also shown in Fig. 5, where the the multiplication factor -bandwidth characteristic is shown for different in Fig. 5(a) and (b). Comparing these figures, the bandwidth of the photodetector decrease by area increasing because of the increase of the photodetectors capacitance. By comparing two Fig. can see bandwidth in WG-SACM- APD specially in low multiplication factor is better than RCE-SAGCM-APD.

In Fig. 6 and Fig. 7 the multiplication factor-bandwidth characteristics of the photodetector is plotted for different the thickness of the absorption layer in both structures.as shown by increasing multiplication layer at first the bandwidth of the photodetector increases because of the decrease of the photodetectors capacitance. However, more increasing cause increases the distance that the photogenerated carriers have to travel, resulting in an increase of the transit time and hence a decrease of the bandwidth of the photodetector.

Also by increasing the thickness of the absorption layer because we have an increase in the transit time so the bandwidth will be decrease.

Comparing these figures, shows the bandwidth of the bandwidth in WG-SACM-APD in low thickness of the absorption layer is better than RCE-SAGCM-APD.

Simulated results shows that decreasing the thickness of the absorption layer increases the bandwidth specially in WG-SACM- APD. However, in RCE-SAGCM-APD decrease thickness of the absorption layer decrease the number of the photogenerated primary carriers and the photocurrent and decrease quantum efficiency .In WG-SACM- APD the equations (14) express decrease thickness of the absorption laye almost no effect on quantum efficiency .So in this structure can reach wide bandwidth with low thickness of the absorption layer and high quantum efficiency with increase the length of the absorption layer.

IV. CONCLUSION

Based on carrier transport equations in RCE-SAGCM-APD and WG-SACM-APD, the corresponding impulse responses have been calculated. The transfer function and then Spice circuit model have been obtained for these devices, based on impulse responses. The parasitic effects also have been included in these circuit models. The bandwidth characteristics curves have been obtained from the proposed models. We have shown that with the variation of device parameters including, thickness of absorption and multiplication layers photodetector area and multiplication one can tune the bandwidth. The comparison between the results of two structures has shown that the bandwidth of waveguide photodetector particularly at small thickness of absorption layer, is higher than the bandwidth of resonant cavity enhanced photodetector. The compromising between quantum efficiency and bandwidth is better performed in waveguide photodetector.

REFERENCES

[1] Y. M. EI-Batawy, M. J. Deen, and N. R. Das," Analysis, Optimization and SPICE Modeling of Resonant Cavity Enhanced PIN Photodetector, 2003, submitted for publication.

[2] J. Wei, F. Xia, and S. R. Forrest, "A high-responsivity high-bandwidth asymmetric twin-waveguide coupled InGaAs-InP- InAlAs avalanche photodiode," ," IEEE Photon.Technol. Lett., vol. 14, no. 11, pp. 1590-1592, Nov. 2002.

3] K. Kishino, M. S. Ünlü, J. Chyi, J. Reed, and H. [Markoç, "Resonant cavity-enhanced (RCE) photodetectors," IEEE J Quantum Electron., vol. 27, pp. 2025-2034, Aug. 1991.

[4] J. A. Jervase and Y. Zebda, "Characteristic analysis of resonant-cavity enhanced (RCE) photodetecors," IEEE J. Quantum Electron., vol. 34, pp. 1129-1134, July 1998.

[5] Y. G. Xiao and M. Jamal Deen,, "Frequency response and modeling of resonant-cavity separate absorption, charge and multiplication avalanche photodiodes," J. Lightwave Tech., vol. 19, pp. 1010-1022, July 2001

[6] Y. M. El-Batawy and M. J. Deen, "Effects of Parasitics on the Time Response of RCE-PDs " IEEE Trans. Electron Devices, vol. 52, pp. 325-334, Mar. 2005

[7] Y. M. El-Batawy and M. J. Deen, "Modeling and optimization of resonant cavity enhanced-separated absorption graded charge multiplication- avalanche photodetector (RCE-SAGCM-APD)," IEEE Trans. Electron Devices, vol. 50, pp. 790-801, Mar. 2003.

[8] Y. M. El-Batawy and M. J. Deen, "Analysis and Circuit Modeling of Waveguide-Separated bsorption Charge Multiplication-Avalanche Photodetector (WG-SACM-APD)" IEEE Trans. Electron Devices, vol. 52, pp. 335-344, Mar. 2005.

[9] Y. M. El-Batawy and M. J. Deen, "Resonant cavity enhanced photodetectors (RCE-PDs), structures, material, analysis and optimization," in Proc. SPIE Quantum Sensing: Evolution and Revolution From Past to Future (Optoelectronics 2003), San Jose, CA, Jan. 2003, pp. 363-378.

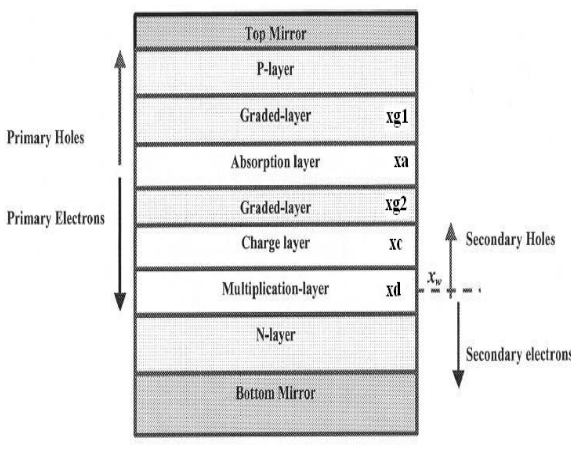

Fig. 1. Schematic representation of RCE-SAGCM-APD.

TABLE I

MATERIAL AND THE VALUES OF BOTH THE PHYSICAL AND CIRCUIT PARAMETERS IN BOTH STRUCTURES

Layer	Material	Thickness (nm)
x_a	InGaAs	35
x_d	InAlAs	80
x_c	InAlAs	50
x_{g1}	InAlAs	210
x_{g2}	InAlAs	50

Layer	Doping (cm^{-3})
n-Layer	4×10^{18}
p-Layer	4×10^{18}
Charge Layer	7×10^{17}

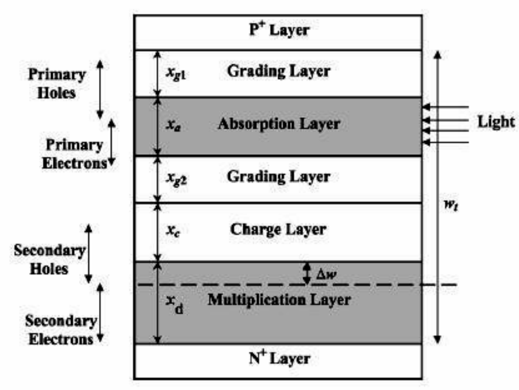

Fig. 2. Schematic of waveguide SACM-APD.

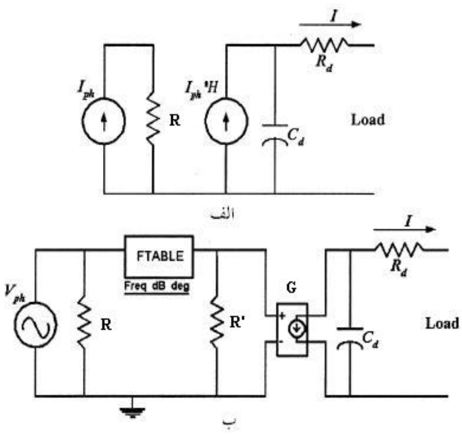

Fig. 3. (a) PSPICE model. (b)PSPICE representation of this model.

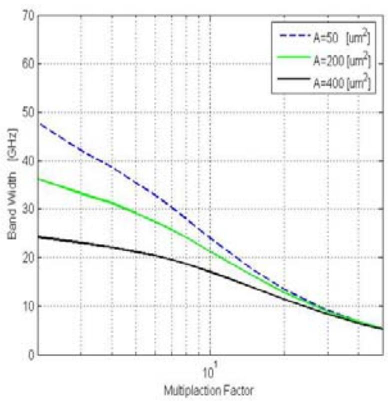

Fig. 4. Bandwidth of the RCE-SAGCM-APD versus the multiplication factor for different areas of the photodetector.

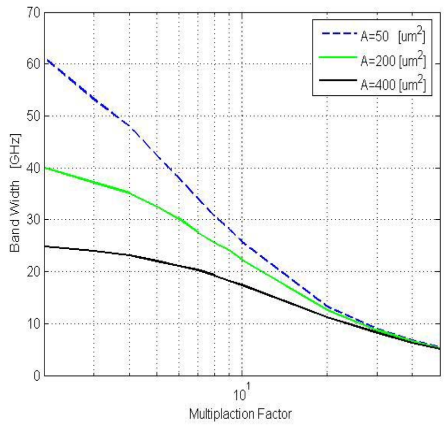

Fig. 5. Bandwidth of the WG-SACM-APD versus the multiplication factor for different areas of the photodetector.

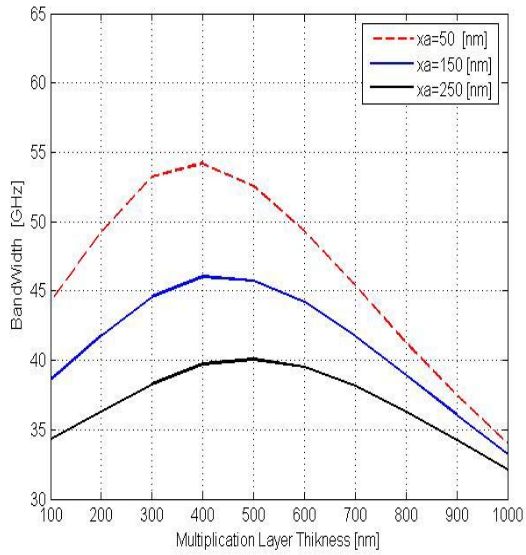

Fig. 6. Bandwidth of the RCE-SAGCM-APD versus the thickness of the multiplication layer factor for different of the absorption layer

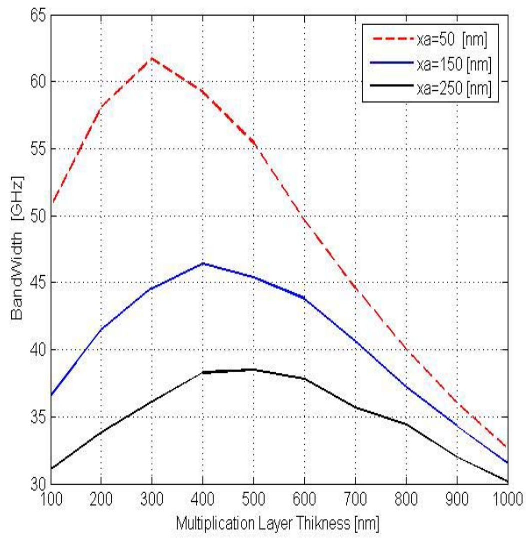

Fig. 6. Bandwidth of the WG-SACM-APD versus the thickness of the multiplication layer factor for different of the absorption layer